SUPPORTING INFORMATION

Covalent inhibitors of *Plasmodium falciparum* glyceraldehyde 3-phosphate dehydrogenase with antimalarial activity in vitro

Gregorio Cullia,[a] Stefano Bruno, [b] Silvia Parapini,[c] Marilena Margiotta,[b] Lucia Tamborini, [a] Andrea Pinto,[d] Andrea Galbiati,[a] Andrea Mozzarelli,[b] Marco Persico,[e] Antonella Paladino,[f] Caterina Fattorusso,[e*] Donatella Taramelli,[g] and Paola Conti[a*]

[a]Dipartimento di Scienze Farmaceutiche, Università degli Studi di Milano, Via Mangiagalli 25, 20133 Milano, Italy. [b]Dipartimento di Scienze degli Alimenti e del Farmaco, Università degli Studi di Parma, Area Parco delle Scienze 23A, 43124, Parma, Italy. [c]Dipartimento di Scienze Biomediche, Chirurgiche e Odontoiatriche, Università degli Studi di Milano, Via Pascal 36, 20133 Milano, Italy. [d]Dipartimento di Scienze per gli Alimenti, la Nutrizione e l'Ambiente, Via Celoria 2, 20133 Milano, Italy. [e]Dipartimento di Farmacia, Università degli Studi di Napoli Federico II, Via D. Montesano 49, 80131 Napoli, Italy. [f]Istituto di Chimica del Riconoscimento Molecolare, Consiglio Nazionale delle Ricerche, Via M. Bianco 9, 20131 Milano, Italy. [g]Dipartimento di Scienze Farmacologiche e Biomolecolari, Università degli Studi di Milano, Via Pascal 36, 20133 Milano.

TABLE OF CONTENTS

1. Materials and methods **3**

1.1 Reagents **3**

1.2 Synthetic procedures and compound characterization **3**

1.3 Biological assays **16**

1.4 Molecular modeling **18**

2. References **22**

3. Figures **24**

4. Tables **32**

1. Materials and methods

1.1 Reagents

Reagents were purchased from Sigma-Aldrich or TCI Europe, unless otherwise specified. Compounds (α*S*,5*S*)-**1a-c**, (α*S*,5*S*)-**5**, and (α*R*,5*S*)-**7** were synthesized according to published procedures.[1,2] DL-glyceraldehyde-3-phosphate was prepared by hydrolysis of DL-glyceraldehyde-3-phosphate diethyl acetal barium salt. Stocks at 34 mM concentration were frozen in small aliquots at −80 °C.

1.2 Synthetic procedures and compound characterization

General

^{1}H NMR and ^{13}C NMR spectra were recorded with a Varian Mercury 300 (300 MHz) spectrometer. Chemical shifts (δ) are expressed in ppm and coupling constants (*J*) in Hz. MS analyses were performed on a Varian 320-MS triple quadrupole mass spectrometer with ESI source. All the synthetic intermediates were at least 90% pure as judged by NMR. The purity of the final compounds was assessed by elemental analysis carried out on a Carlo Erba model 1106 (elemental analyzer for C, H and N), and the results were within ±0.4% of the theoretical values. Rotary power determinations were carried out using a Jasco P-1010 spectropolarimeter, coupled with a Haake N3-B thermostat. TLC analyses were performed on commercial silica gel 60 F254 aluminum sheets; spots were further evidenced by spraying with a dilute alkaline solution of $KMnO_4$ or with ninhydrin. Melting points were determined on a model B 540 Büchi apparatus and are uncorrected.

General procedure for the synthesis of compounds 6a-e

Amine (1 eq), EDC hydrochloride (1 eq) and HOBt (0.5 eq.) were added to a 0.028 M solution of (α*S*,5*S*)-**5** (1 eq.) in THF. The reaction mixture was stirred at room temperature for 2 h, then the solvent was removed under reduced pressure and the crude product was purified by flash chromatography on silica gel (cyclohexane/EtOAc, 7:3 v/v).

Synthesis of *tert*-butyl (*S*)-2-(benzylamino)-1-((*S*)-3-bromo-4,5-dihydroisoxazol-5-yl)-2-oxoethylcarbamate [(α*S*,5*S*)-6a]

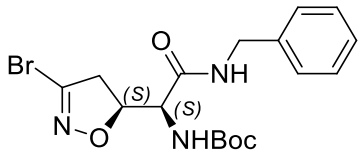

(α*S*,5*S*)-**6a**

The product was obtained following the general procedure for the synthesis of compounds **6a-e**. *tert*-Butyl (*S*)-2-(benzylamino)-1-((*S*)-3-bromo-4,5-dihydroisoxazol-5-yl)-2-oxoethylcarbamate [(α*S*,5*S*)-**6a**] was obtained as colourless oil (48 mg, 70% yield). R_f 0.32 (cyclohexane/EtOAc, 7:3 v/v). ^{1}H NMR (300 MHz, $CDCl_3$): δ 7.38-7.22 (m, 5H), 6.54 (t, *J* = 5.7 Hz, 1H), 5.48 (d, *J* = 7.8 Hz, 1H), 4.74 (ddd, *J* = 6.6, 8.3, 10.5 Hz, 1H), 4.48 (d, *J* = 5.7 Hz, 2H), 4.26 (dd, *J* = 7.8, 8.3 Hz, 1H), 3.52 (dd, *J* = 6.6, 17.7 Hz, 1H), 3.32 (dd, *J* = 10.5, 17.7 Hz, 1H), 1.44 (s, 9H). ^{13}C NMR (75 MHz, $CDCl_3$): δ 168.4, 155.9, 138.8, 137.4, 128.7, 127.6, 127.6, 81.8, 80.8, 55.7, 44.3, 43.8, 28.2. $[\alpha]_D^{20}$ + 141.3 (*c* 1.0, $CHCl_3$).

Synthesis of *tert*-butyl (*S*)-1-((*S*)-3-bromo-4,5-dihydroisoxazol-5-yl)-2-(4-methoxybenzylamino)-2-oxoethylcarbamate [(α*S*,5*S*)-6b]

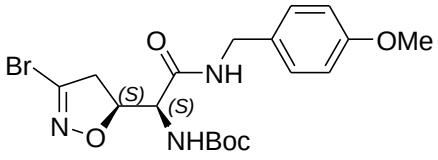

(α*S*,5*S*)-**6b**

The product was obtained following the general procedure for the synthesis of compounds **6a-e**. *tert*-Butyl (*S*)-1-((*S*)-3-bromo-4,5-dihydroisoxazol-5-yl)-2-(4-methoxybenzylamino)-2-oxoethyl-carbamate [(α*S*,5*S*)-**6b**] was obtained as white foam (93 mg, 68% yield). R_f 0.30 (cyclohexane/EtOAc, 7:3 v/v). ^{1}H NMR (300 MHz, $CDCl_3$): δ 7.20 (m, 2H), 6.86 (m, 2H), 6.47 (t, *J* = 5.7 Hz, 1H), 5.47 (d, *J* = 8.4 Hz, 1H), 4.72 (ddd, *J* = 6.6, 7.5, 10.5 Hz, 1H), 4.40 (d, *J* = 5.7 Hz, 2H), 4.24 (dd, *J* = 7.5, 8.4 Hz, 1H), 3.79 (s, 3H), 3.51 (dd, *J* = 6.6, 17.6 Hz, 1H), 3.31 (dd, *J* = 10.5, 17.6 Hz, 1H), 1.43 (s, 9H). ^{13}C NMR (75 MHz, $CDCl_3$): δ 168.4, 159.0, 155.8, 138.6, 129.6, 129.0, 114.1, 81.8, 80.7, 55.7, 55.3, 44.1, 43.2, 28.2. $[\alpha]_D^{20}$ + 135.8 (*c* 0.50, $CHCl_3$).

Synthesis of *tert*-butyl (*S*)-1-((*S*)-3-bromo-4,5-dihydroisoxazol-5-yl)-2-(4-fluorobenzylamino)-2-oxoethylcarbamate [(α*S*,5*S*)-6c]

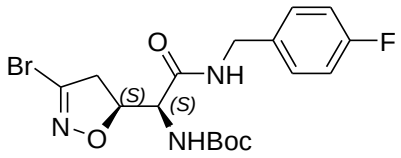

(α*S*,5*S*)-**6c**

The product was obtained following the general procedure for the synthesis of compounds **6a-e**. *tert*-Butyl (*S*)-1-((*S*)-3-bromo-4,5-dihydroisoxazol-5-yl)-2-(4-fluorobenzylamino)-2-oxoethyl carbamate [(α*S*,5*S*)-**6c**] was obtained as brown oil (103 mg, 77% yield). R_f 0.27 (cyclohexane/EtOAc, 7:3 v/v). ^{1}H NMR (300 MHz, $CDCl_3$): δ 7.24 (m, 2H), 7.01 (m, 2H), 6.55 (t, *J* = 5.7 Hz, 1H), 5.46 (d, *J* = 6.6 Hz, 1H), 4.73 (m, 1H), 4.44 (d, *J* = 5.7 Hz, 2H), 4.25 (t, *J* = 7.9 Hz, 1H), 3.52 (dd, *J* = 5.8, 17.7 Hz, 1H), 3.32 (dd, *J* = 10.9, 17.7 Hz, 1H), 1.44 (s, 9H). ^{13}C NMR (75 MHz, $CDCl_3$): δ 168.5, 162.2 (d, $^1J_{C\text{-}F}$ = 243.9 Hz), 155.8, 138.7, 133.3 (d, $^4J_{C\text{-}F}$ = 2.8 Hz), 129.3 (d, $^3J_{C\text{-}F}$ = 9.1 Hz), 115.5 (d, $^2J_{C\text{-}F}$ = 21.7 Hz), 81.7, 80.8, 55.7, 44.2, 43.0, 28.2. $[\alpha]_D^{20}$ + 94.9 (*c* 0.50, $CHCl_3$).

Synthesis of *tert*-butyl (*S*)-1-((*S*)-3-bromo-4,5-dihydroisoxazol-5-yl)-2-(4-nitrobenzylamino)-2-oxoethylcarbamate [(α*S*,5*S*)-6d]

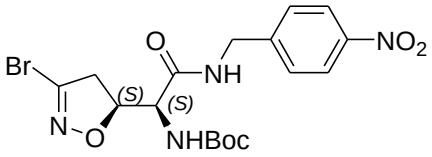

(α*S*,5*S*)-**6d**

The product was obtained following the general procedure for the synthesis of compounds **6a-e**. *tert*-Butyl (*S*)-1-((*S*)-3-bromo-4,5-dihydroisoxazol-5-yl)-2-(4-nitrobenzylamino)-2-oxoethyl carbamate [(α*S*,5*S*)-**6d**] was obtained as yellow solid (90 mg, 64% yield) which recrystallizes from 1:4 v/v *i*PrOH/*n*-hexane as colorless needles (m.p. 140.8-141.5 °C). R_f 0.26 (cyclohexane/EtOAc, 7:3 v/v). ^{1}H NMR (300 MHz, $CDCl_3$): δ 8.18 (d, *J* = 8.5 Hz, 2H), 7.45 (d, *J* = 8.5 Hz, 2H), 6.92 (t, *J* = 5.7 Hz, 1H), 5.48 (d, *J* = 7.5 Hz, 1H), 4.77 (ddd, *J* = 6.0, 6.3, 10.5 Hz, 1H), 4.61 (dd, *J* = 6.6, 15.9 Hz, 1H), 4.54 (dd, *J* = 6.0, 15.9 Hz, 1H), 4.33 (dd, *J* = 6.0, 7.5 Hz, 1H), 3.52 (dd, *J* = 6.3, 18.1 Hz, 1H), 3.34 (dd, *J* = 10.5, 18.1 Hz, 1H), 1.44 (s, 9H). ^{13}C NMR (75 MHz, $CDCl_3$): δ 169.1, 155.9, 147.2, 145.2, 138.8, 128.0, 123.8, 81.6, 81.0, 55.8, 44.2, 42.9, 28.2. $[\alpha]_D^{20}$ + 102.6 (*c* 0.50, $CHCl_3$).

Synthesis of *tert*-butyl ((*S*)-1-((*S*)-3-bromo-4,5-dihydroisoxazol-5-yl)-2-oxo-2-(phenethylamino)ethyl)carbamate [(α*S*,5*S*)-6e]

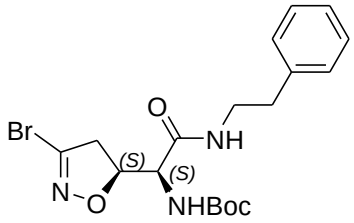

(α*S*,5*S*)-**6e**

The product was obtained following the general procedure for the synthesis of compounds **6a-e**. *tert*-Butyl ((*S*)-1-((*S*)-3-bromo-4,5-dihydroisoxazol-5-yl)-2-oxo-2-(phenethylamino)ethyl)carbamate [(α*S*,5*S*)-**6e**] was obtained as yellow oil (107 mg, 81% yield). R_f 0.31 (cyclohexane/EtOAc, 7:3 v/v). ^{1}H NMR (300 MHz, $CDCl_3$): δ 7.36-7.15 (m, 5H), 6.23 (t, *J* = 5.2 Hz, 1H), 5.39 (d, *J* = 7.6 Hz, 1H), 4.65 (ddd, *J* = 6.7, 7.8, 10.6 Hz, 1H), 4.16 (t, *J* = 8.1 Hz, 1H), 3.64-3.46 (m, 2H), 3.46 (dd, *J* = 6.7, 17.7 Hz, 1H), 3.26 (dd, *J* = 10.6, 17.7Hz, 1H), 2.82 (t, *J* = 7.1 Hz, 2H), 1.44 (s, 9H). ^{13}C NMR (75 MHz, $CDCl_3$): δ 168.4, 155.8, 138.6, 138.5, 128.7, 128.6, 126.5, 81.8, 80.7, 55.6, 44.0, 41.0, 35.6, 28.2. $[\alpha]_D^{20}$ + 109.7 (*c* 0.50, $CHCl_3$).

General procedure for the synthesis of compounds 2a-e

Compound **6a-e** (1 eq.) was treated with a 15% TFA/DCM solution (10 eq) at room temperature until complete deprotection (normally between 2 and 4 h), then it was diluted with DCM and the acid was quenched with 5% aq. $NaHCO_3$. Phases were separated and the aqueous phase was extracted with DCM. The pooled organic layers were dried over anhydrous Na_2SO_4, filtered and the solvent was removed under reduced pressure. The crude product was purified by flash chromatography on silica gel (EtOAc, 100%).

Synthesis of (*S*)-2-amino-*N*-benzyl-2-((*S*)-3-bromo-4,5-dihydroisoxazol-5-yl)acetamide [(α*S*,5*S*)-2a]

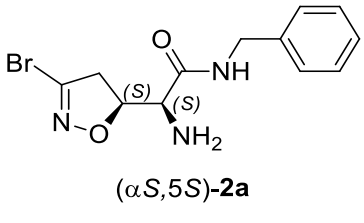

(α*S*,5*S*)-**2a**

The product was obtained following the general procedure for the synthesis of compounds **2a-e**. (*S*)-2-Amino-*N*-benzyl-2-((*S*)-3-bromo-4,5-dihydroisoxazol-5-yl)acetamide [(α*S*,5*S*)-**2a**] was obtained as colourless solid (55 mg, 73% yield), which recrystallizes from 1:3 v/v *i*PrOH/*n*-hexane as colourless needles (m.p. 90.6-91.3 °C). R_f 0.28 (EtOAc, 100%). ^{1}H NMR (300 MHz, $CDCl_3$): δ

7.41-7.23 (m, 6H), 5.09 (dt, *J* = 4.8, 9.6 Hz, 1H), 4.44 (d, *J* = 6.3 Hz, 2H), 3.80 (d, *J* = 4.8 Hz, 1H), 3.22 (d, *J* = 9.6 Hz, 2H), 1.49 (bs, 2H). ^{13}C NMR (75 MHz, $CDCl_3$): δ 170.5, 138.1, 137.8, 128.8, 127.7, 127.6, 82.8, 56.4, 43.3, 41.8. $[\alpha]_D^{20}$ + 80.9 (*c* 1.0, $CHCl_3$). MS(ESI): *m/z* calcd for $C_{12}H_{14}BrN_3O_2$: 311.0; found: 311.9 $[M+H]^+$. Anal. calcd for $C_{12}H_{14}BrN_3O_2$: C 46.17, H 4.52, N 13.46, found: C 45.96, H 4.57, N 13.36.

Synthesis and (*S*)-2-amino-2-((*S*)-3-bromo-4,5-dihydroisoxazol-5-yl)-*N*-(4-methoxybenzyl)acetamide [(α*S*,5*S*)-2b]

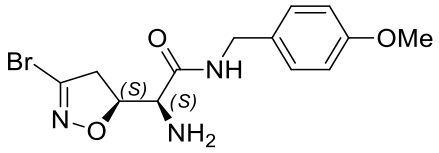

(α*S*,5*S*)-**2b**

The product was obtained following the general procedure for the synthesis of compounds **2a-e**. (*S*)-2-Amino-2-((*S*)-3-bromo-4,5-dihydroisoxazol-5-yl)-*N*-(4-methoxybenzyl)acetamide [(α*S*,5*S*)-**2b**] was obtained as colourless solid (58 mg, 84% yield) which recrystallizes from 1:3 v/v *i*PrOH/*n*-hexane as colourless needles (m.p. 118.0-118.8 °C). R_f 0.31 (EtOAc, 100%). ^{1}H NMR (300 MHz, CD_3OD): δ 7.22 (d, *J* = 8.1 Hz, 2H), 6.86 (d, *J* = 8.1 Hz, 2H), 4.32 (s, 2H), 3.76 (s, 3H), 3.55 (d, *J* = 5.7 Hz, 1H). ^{13}C NMR (75 MHz, CD_3OD): δ 171.9, 159.0, 138.0, 130.1, 128.5, 113.5, 83.0, 56.5, 54.3, 42.2, 42.1. $[\alpha]_D^{20}$ + 143.0 (*c* 0.50, MeOH). MS(ESI): *m/z* calcd for $C_{13}H_{16}BrN_3O_3$: 341.0; found: 342.1 $[M+H]^+$. Anal. calcd for $C_{13}H_{16}BrN_3O_3$: C 45.63, H 4.71, N 12.28, found: C 45.32, H 4.77, N 12.17.

Synthesis of (*S*)-2-amino-2-((*S*)-3-bromo-4,5-dihydroisoxazol-5-yl)-*N*-(4-fluorobenzyl)acetamide [(α*S*,5*S*)-2c]

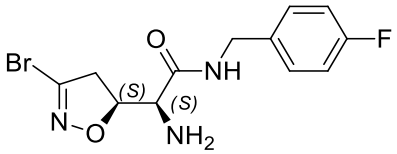

(α*S*,5*S*)-**2c**

The product was obtained following the general procedure for the synthesis of compounds **2a-e**. (*S*)-2-Amino-2-((*S*)-3-bromo-4,5-dihydroisoxazol-5-yl)-*N*-(4-fluorobenzyl)acetamide [(α*S*,5*S*)-**2c**] was obtained as colourless solid (46 mg, 55% yield) which recrystallizes from 1:4 v/v *i*PrOH/*n*-hexane as white needles (m.p. 86.2-86.6 °C). R_f 0.44 (EtOAc, 100%). ^{1}H NMR (300 MHz, $CDCl_3$):

δ 7.38, (t, *J* = 6.0 Hz, 1H), 7.24 (m, 2H), 7.02 (m, 2H), 5.07 (dt, *J* = 4.5, 10.0 Hz, 1H), 4.41 (d, *J* = 6.0 Hz, 2H), 3.80 (d, *J* = 4.5 Hz, 1H), 3.23 (d, *J* = 10.0 Hz, 2H), 1.73 (bs, 2H). ^{13}C NMR (75 MHz, $CDCl_3$): δ 170.7, 162.2 (d, $^{1}J_{C\text{-}F}$ = 245.0 Hz), 138.1, 133.7 (d, $^{4}J_{C\text{-}F}$ = 3.0 Hz), 129.4 (d, $^{3}J_{C\text{-}F}$ = 8.0 Hz), 115.6 (d, $^{2}J_{C\text{-}F}$ = 20.6 Hz), 82.7, 56.4, 42.6, 42.0. $[\alpha]_D^{20}$ + 86.1 (*c* 0.50, $CHCl_3$). MS(ESI): *m/z* calcd for $C_{12}H_{13}BrFN_3O_2$: 329.0; found: 329.9 $[M+H]^+$. Anal. calcd for $C_{12}H_{13}BrFN_3O_2$: C 43.66, H 3.97, N 12.73, found: C 43.38, H 4.05, N 12.61.

Synthesis of (*S*)-2-amino-2-((*S*)-3-bromo-4,5-dihydroisoxazol-5-yl)-*N*-(4-nitrobenzyl)acetamide [(α*S*,5*S*)-2d]

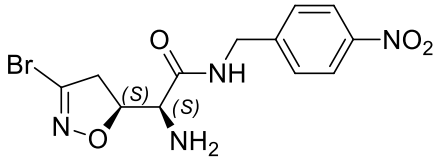

(α*S*,5*S*)-**2d**

The product was obtained following the general procedure for the synthesis of compounds **2a-e**. (*S*)-2-Amino-2-((*S*)-3-bromo-4,5-dihydroisoxazol-5-yl)-*N*-(4-nitrobenzyl)acetamide [(α*S*,5*S*)-**2d**] was obtained as colourless solid (51 mg, 76% yield) which recrystallizes from 1:3 v/v *i*PrOH/*n*-hexane as white needles (m.p. 138.8-139.3 °C). R_f 0.30 (EtOAc, 100%). ^{1}H NMR (300 MHz, CD_3OD): δ 8.18 (m, 2H), 7.54 (m, 2H), 4.85 (dt, *J* = 6.0, 9.6 Hz, 1H), 4.56 (d, *J* = 16.0 Hz, 1H), 4.48 (d, *J* = 16.0 Hz, 1H), 3.57 (d, *J* = 6.0 Hz, 1H), 3.36 (d, *J* = 9.6 Hz, 2H). ^{13}C NMR (75 MHz, CD_3OD): δ 172.7, 147.1, 146.2, 138.1, 127.9, 123.2, 83.1, 56.8, 42.6, 42.0. $[\alpha]_D^{20}$ + 112.0 (*c* 0.33, MeOH). MS(ESI): *m/z* calcd for $C_{12}H_{13}BrN_4O_4$: 356.0; found: 357.0 $[M+H]^+$. Anal. calcd for $C_{12}H_{13}BrN_4O_4$: C 40.35, H 3.67, N 15.69, found: C 40.12, H 3.79, N 15.47.

Synthesis of (*S*)-2-amino-2-((*S*)-3-bromo-4,5-dihydroisoxazol-5-yl)-*N*-phenethylacetamide [(α*S*,5*S*)-2e]

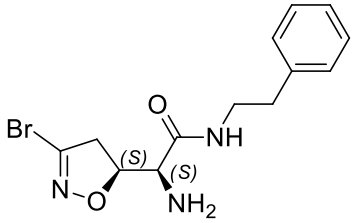

(α*S*,5*S*)-**2e**

The product was obtained following the general procedure for the synthesis of compounds **2a-e**. (*S*)-2-amino-2-((*S*)-3-bromo-4,5-dihydroisoxazol-5-yl)-*N*-phenethylacetamide [(α*S*,5*S*)-**2e**] was

obtained as yellow oil (39 mg, 51% yield). R_f 0.24 (EtOAc, 100%). ^{1}H NMR (300 MHz, $CDCl_3$): δ 7.38-7.16 (m, 5H), 7.07 (t, *J* = 6.6 Hz, 1H), 5.02 (ddd, *J* = 4.3, 9.0, 10.7 Hz, 1H), 3.75 (d, *J* = 4.3 Hz, 1H), 3.61 (m, 1H), 3.51 (m, 1H), 3.09-2.75 (m, 4H), 1.58 (bs, 2H). ^{13}C NMR (75 MHz, $CDCl_3$): δ 170.3, 138.5, 138.1, 128.7, 128.7, 126.7, 82.6, 56.3, 41.3, 40.1, 35.5. $[\alpha]_D^{20}$ + 93.8 (*c* 0.36, $CHCl_3$). MS(ESI): *m/z* calcd for $C_{13}H_{16}BrN_3O_2$: 325.0; found: 326.1 $[M+H]^+$. Anal. calcd for $C_{13}H_{16}BrN_3O_2$: C 47.87, H 4.94, N 12.88, found: C 48.19, H 5.13, N 12.67.

Synthesis of *tert*-butyl (*R*)-2-(benzyloxy)-1-((*S*)-3-bromo-4,5-dihydroisoxazol-5-yl)ethylcarbamate [(α*R*,5*S*)-8]

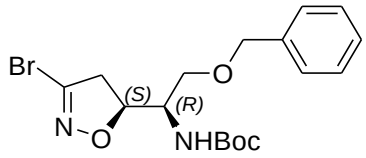

(α*R*,5*S*)-**8**

Freshly prepared Ag_2O (115 mg, 0.498 mmol) and benzyl bromide (395 µL, 3.32 mmol) were added to a solution of (α*R*,5*S*)-**7** (100 mg, 0.332 mmol) in DCM (4.0 mL). Reaction mixture was stirred at room temperature overnight, then it was filtered over celite and the solvent was removed under reduced pressure. The crude product was purified by flash chromatography on silica gel (cyclohexane/EtOAc, 9:1 to 8:2 v/v) obtaining *tert*-butyl (*R*)-2-(benzyloxy)-1-((*S*)-3-bromo-4,5-dihydroisoxazol-5-yl)ethylcarbamate [(α*R*,5*S*)-**8**] as yellow oil (48 mg, 36% yield). R_f 0.50 (cyclohexane/EtOAc, 8:2 v/v). ^{1}H NMR (300 MHz, $CDCl_3$): δ 7.41-7.25 (m, 5H), 5.06 (d, *J* = 7.1 Hz, 1H), 4.77 (ddd, *J* = 7.2, 8.4, 10.2 Hz, 1H), 4.52 (s, 2H), 3.85 (m, 1H), 3.79 (dd, *J* = 2.5, 9.6 Hz, 1H), 3.55 (dd, *J* = 3.7, 9.6 Hz, 1H), 3.34 (dd, *J* = 7.2, 17.7 Hz, 1H), 3.22 (dd, *J* = 10.2, 17.7 Hz, 1H), 1.44 (s, 9H). ^{13}C NMR (75 MHz, $CDCl_3$): δ 155.6, 138.0, 137.7, 128.5, 127.9, 127.7, 80.6, 80.1, 73.5, 68.6, 52.4, 44.3, 28.3. $[\alpha]_D^{20}$ + 48.0 (*c* 0.95, $CHCl_3$).

Synthesis of (*R*)-2-(benzyloxy)-1-((*S*)-3-bromo-4,5-dihydroisoxazol-5-yl)ethanamine [(α*R*,5*S*)-3a]

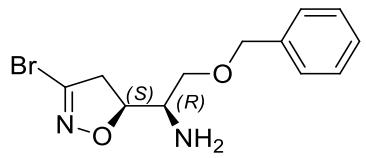

(α*R*,5*S*)-**3a**

(α*R*,5*S*)-**8** (45 mg, 0.113 mmol) was treated with 15% TFA/DCM (573 µL, 10 eq). at room temperature for 4 h, then DCM was added and the acid was quenched with 5% aq. $NaHCO_3$. Phases

were separated and the aqueous phase was extracted with DCM. The pooled organic layers were dried over anhydrous Na_2SO_4, filtered and the solvent was removed under reduced pressure. The crude product was purified by flash chromatography on silica gel (DCM/MeOH, 96:4 v/v) obtaining (*R*)-2-(benzyloxy)-1-((*S*)-3-bromo-4,5-dihydroisoxazol-5-yl)ethanamine [(α*R*,5*S*)-**3a**] as yellow oil (19 mg, 56% yield). R_f 0.32 (DCM/MeOH, 96:4 v/v). ^{1}H NMR (300 MHz, $CDCl_3$): δ 7.40-7.25 (m, 5H), 4.69 (ddd, *J* = 5.3, 8.7, 10.8 Hz, 1H), 4.51 (s, 2H), 3.50 (dd, *J* = 4.5, 9.3 Hz, 1H), 3.40 (dd, *J* = 5.7, 9.3 Hz, 1H), 3.34 (dd, *J* = 8.7, 17.7 Hz, 1H), 3.28 (ddd, *J* = 4.5, 5.3, 5.7 Hz, 1H), 3.10 (dd, *J* = 10.8, 17.7 Hz, 1H), 1.38 (bs, 2H). ^{13}C NMR (75 MHz, $CDCl_3$): δ 138.0, 137.8, 128.5, 127.8, 127.7, 83.3, 73.5, 71.3, 52.5, 42.3. $[\alpha]_D^{20}$ + 58.3 (*c* 0.75, $CHCl_3$). MS(ESI): *m/z* calcd for $C_{12}H_{15}BrN_2O_2$: 298.0; found: 298.8 $[M+H]^+$. Anal. calcd for $C_{12}H_{15}BrN_2O_2$: C 48.18, H 5.05, N 9.36, found: C 48.26, H 5.28, N 9.11.

Synthesis of (*S*)-*tert*-butyl (1-hydroxybut-3-en-2-yl)carbamate [(*S*)-9]

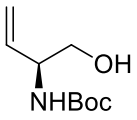

(*S*)-**9**

The product was obtained following a published procedure.[3]

Characterisation is in accordance with literature.[4]

R_f 0.29 (cyclohexane/EtOAc, 6:4 v/v). ^{1}H-NMR (300 MHz, $CDCl_3$): δ 5.79 (ddd, *J* = 5.4, 10.5, 17.1 Hz, 1H), 5.24 (dd, *J* = 1.2, 17.1 Hz, 1H), 5.19 (dd, *J* = 1.2, 10.5 Hz, 1H), 5.00 (d, *J* = 7.2 Hz, 1H), 4.20 (m, 1H), 3.68 (dd, *J* = 4.7, 11.3 Hz, 1H), 3.59 (dd, *J* = 5.9, 11.3 Hz, 1H), 2.62 (m, 1H), 1.43 (s, 9H). ^{13}C-NMR (75 MHz, $CDCl_3$): δ 156.0, 135.5, 116.4, 79.8, 65.0, 54.6, 28.3. $[\alpha]_D^{20}$ − 22.4 (*c* 0.55, $CHCl_3$). (lit. − 22.4)[3]

Synthesis of (*S*)-*tert*-butyl 1-(benzylthio)but-3-en-2-ylcarbamate [(*S*)-10]

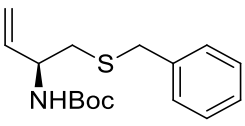

(*S*)-**10**

MsCl (83 µL, 1.07 mmol) was added at 0°C to a solution of (*S*)-**9** (200 mg, 1.07 mmol) was dissolved in dry DCM (2 mL). TEA (194 µL, 1.39 mmol) and DMAP (13 mg, 0.107 mmol). The reaction mixture was stirred at 0°C for 15 min, then it was diluted with DCM, washed with 1 M aq.

HCl and sat. aq. $NaHCO_3$. The organic phase was dried over anhydrous Na_2SO_4, filtered and the solvent was removed under reduced pressure, obtaining (*S*)-2-(*tert*-butoxycarbonylamino)but-3-enyl methanesulfonate as yellow oil (256 mg, 90% yield). R_f 0.51 (cyclohexane/EtOAc, 6:4 v/v). ^{1}H NMR (300 MHz, $CDCl_3$): δ 5.80 (ddd, *J* = 6.0, 10.5, 17.1 Hz, 1H), 5.31 (d, *J* = 17.1 Hz, 1H), 5.27 (d, *J* = 10.5 Hz, 1H), 4.82 (m, 1H), 4.45 (m, 1H), 4.29 (dd, *J* = 4.5, 10.2 Hz, 1H), 4.21 (dd, *J* = 5.3, 10.2 Hz, 1H), 3.02 (s, 3H), 1.44 (s, 9H). ^{13}C NMR (75 MHz, $CDCl_3$): δ 155.0, 133.6, 117.8, 80.2, 70.5, 51.7, 37.5, 28.3. $[\alpha]_D^{20}$ − 33.7 (*c* 0.50, $CHCl_3$).

Phenylmethanethiol (113 µL, 0.965 mmol) and DBU (217 µL, 1.45 mmol) were added to a solution of (*S*)-2-(*tert*-butoxycarbonylamino)but-3-enyl methanesulfonate (256 mg, 0.965 mmol) in benzene (1.2 mL). Reaction mixture was stirred at room temperature for 1 h and additional phenylmethanethiol (23 µL, 0.193 mmol) was added. The reaction mixture was stirred for 30 min then Et_2O was added and washed two times with 0.2 M aq. NaOH. The aqueous phase was extracted with Et_2O and the pooled organic phases were washed with brine, dried over anhydrous Na_2SO_4, filtered and the solvent was removed under reduced pressure. The crude product was purified by flash chromatography on silica gel (cyclohexane/EtOAc, 95:5 to 9:1 v/v) obtaining (*S*)-*tert*-butyl 1-(benzylthio)but-3-en-2-ylcarbamate [(*S*)-**10**] as colourless oil (226 mg, 80% yield). R_f 0.32 (cyclohexane/EtOAc, 9:1 v/v). ^{1}H NMR (300 MHz, $CDCl_3$): δ 7.35-7.19 (m, 5H), 5.78 (ddd, *J* = 5.4, 11.1, 17.1 Hz, 1H), 5.19 (d, *J* = 17.1 Hz, 1H), 5.14 (d, *J* = 11.1 Hz, 1H), 4.74 (m, 1H), 4.33 (m, 1H), 3.73 (s, 2H), 2.59 (d, *J* = 6.3 Hz, 2H), 1.45 (s, 9H). ^{13}C NMR (75 MHz, $CDCl_3$): δ 155.2, 138.0, 137.4, 128.9, 128.5, 127.1, 115.5, 79.6, 51.7, 36.7, 36.4, 28.4. $[\alpha]_D^{20}$ − 11.8 (*c* 1.00, $CHCl_3$).

Synthesis of *tert*-butyl (*S*)-2-(benzylthio)-1-((*S*)-3-bromo-4,5-dihydroisoxazol-5-yl)ethylcarbamate [(α*S*,5*S*)-11] and *tert*-butyl (*S*)-2-(benzylthio)-1-((*R*)-3-bromo-4,5-dihydroisoxazol-5-yl)ethylcarbamate [(α*S*,5*R*)-12]

DBF (187 mg, 0.924 mmol) and $NaHCO_3$ (388 mg, 4.62 mmol) were added to a solution of (*S*)-**9** (226 mg, 0.770 mmol) in EtOAc (4 mL). The reaction mixture was vigorously stirred at room temperature until consumption of (*S*)-**10**. EtOAc was added, washed with water, dried over anhydrous Na_2SO_4, filtered and the solvent was removed under reduced pressure. The crude product was purified by flash chromatography on silica gel (cyclohexane/EtOAc, 9:1 to 85:15 v/v).

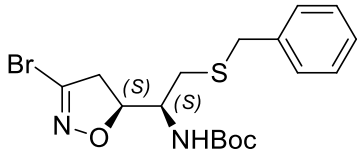

(α*S*,5*S*)-**11**

tert-Butyl (*S*)-2-(benzylthio)-1-((*S*)-3-bromo-4,5-dihydroisoxazol-5-yl)ethylcarbamate [(α*S*,5*S*)-**11**] was obtained as green oil (138 mg, 43% yield) which solidifies upon cooling at − 20 °C. R_f 0.15 (cyclohexane/EtOAc, 9:1 v/v). ^{1}H NMR (300 MHz, $CDCl_3$): δ 7.35-7.20 (m, 6H), 4.79 (d, *J* = 9.3 Hz, 1H), 4.65 (ddd, *J* = 7.6, 7.8, 10.2 Hz, 1H), 3.83 (m, 1H), 3.73 (s, 2H), 3.23 (dd, *J* = 10.2, 17.7 Hz, 1H), 3.11 (dd, *J* = 7.6, 17.7 Hz, 1H), 2.67 (d, *J* = 5.7 Hz, 2H), 1.45 (s, 9H). ^{13}C NMR (75 MHz, $CDCl_3$): δ 155.5, 137.7, 137.7, 129.0, 128.6, 127.3, 82.3, 80.2, 52.3, 44.4, 36.8, 32.2, 28.3. $[\alpha]_D^{20}$ + 84.6 (*c* 1.05, $CHCl_3$).

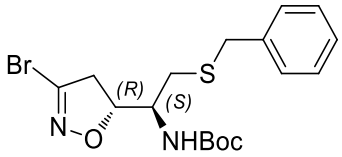

(α*S*,5*R*)-**12**

tert-Butyl (*S*)-2-(benzylthio)-1-((*R*)-3-bromo-4,5-dihydroisoxazol-5-yl)ethylcarbamate[(α*S*,5*R*)-**12**] was obtained as a white solid (164 mg, 51% yield) which recrystallizes from diisopropylether as white needles (m.p. 106.5-107.3 °C). R_f 0.22 (cyclohexane/EtOAc, 9:1 v/v). ^{1}H NMR (300 MHz, $CDCl_3$): δ 7.37-7.20 (m, 5H), 4.98 (ddd, *J* = 1.8, 8.4, 11.1 Hz, 1H), 4.66 (d, *J* = 9.9 Hz, 1H), 3.87 (dt, *J* = 7.8, 8.4 Hz, 1H), 3.73 (s, 2H), 3.25 (dd, *J* = 11.1, 17.4 Hz, 1H), 3.10 (dd, *J* = 8.4, 17.4 Hz, 1H), 2.57 (d, *J* = 7.8 Hz, 2H), 1.45 (s, 9H). ^{13}C NMR (75 MHz, $CDCl_3$): δ 156.0, 138.2, 137.8, 129.0, 128.5, 127.2, 81.0, 80.2, 52.2, 44.0, 36.1, 33.0, 28.3. $[\alpha]_D^{20}$ − 85.5 (*c* 1.00, $CHCl_3$).

Synthesis of (*S*)-2-(benzylthio)-1-((*S*)-3-bromo-4,5-dihydroisoxazol-5-yl)ethan-1-amine [(α*S*,5*S*)-3b]

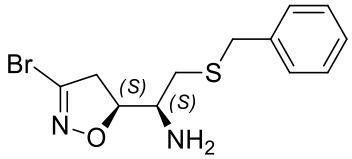

(α*S*,5*S*)-**3b**

(α*S*,5*S*)-**11** (83 mg, 0.20 mmol) was treated with 15% TFA/DCM (1.0 mL, 10 eq) at room temperature for 4 h, then it was diluted with DCM and the acid was quenched with 5% aq.

$NaHCO_3$. Phases were separated and the aqueous phase was extracted with DCM. The pooled organic layers were dried over anhydrous Na_2SO_4, filtered and the solvent was removed under reduced pressure. The crude product was purified by flash chromatography on silica gel (cyclohexane/EtOAc, 2:8 v/v) obtained (*S*)-2-(benzylthio)-1-((*S*)-3-bromo-4,5-dihydroisoxazol-5-yl)ethan-1-amine [(α*S*,5*S*)-**3b**] as yellow oil (48mg, 76% yield). R_f 0.42 (cyclohexane/EtOAc, 6:4 v/v). ^{1}H NMR (300 MHz, $CDCl_3$): δ 7.41-7.20 (m, 5H), 4.58 (ddd, *J* = 5.0, 8.5, 10.7 Hz, 1H), 3.72 (s, 2H), 3.24 (dd, *J* = 8.5, 17.2 Hz, 1H), 3.16 (ddd, *J* = 4.2, 5.0, 8.8 Hz, 1H), 3.05 (dd, *J* = 10.7, 17.2 Hz, 1H), 2.56 (dd, *J* = 4.2, 13.5 Hz, 1H), 2.29 (dd, *J* = 8.8, 13.5 Hz, 1H), 1.49 (bs, 2H). ^{13}C NMR (75 MHz, $CDCl_3$): δ 137.8, 137.8, 128.9, 128.6, 127.3, 84.6, 51.5, 41.9, 36.4, 34.8. $[\alpha]_D^{20}$ + 57.7 (*c* 0.66, $CHCl_3$). MS(ESI): *m/z* calcd for $C_{12}H_{15}BrN_2OS$: 314.0; found: 315.0 $[M+H]^+$. Anal. calcd for $C_{12}H_{15}BrN_2OS$: C 45.72, H 4.80, N 8.89, found: C 45.88, H 4.90, N 8.57.

Synthesis of (*S*)-2-(benzylsulfonyl)-1-((*S*)-3-bromo-4,5-dihydroisoxazol-5-yl)ethanamine [(α*S*,5*S*)-3c]

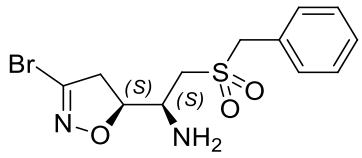

(α*S*,5*S*)-**3c**

*m*CPBA (214 mg, ≥77% purity, 0.953 mmol) was added at 0°C to a solution of [(α*S*,5*S*)-**11**] (180 mg, 0.433 mmol) in $CHCl_3$ (5.3 mL). Reaction mixture was stirred at room temperature for 10 min then DCM was added and washed with sat. aq. $NaHCO_3$. The organic phase was dried over anhydrous Na_2SO_4, filtered and the solvent was removed under reduced pressure. The crude was decanted from 1:1 v/v cyclohexane/EtOAc as eluent, obtaining *tert*-butyl (*S*)-2-(benzylsulfonyl)-1-((*S*)-3-bromo-4,5-dihydroisoxazol-5-yl)ethylcarbamate as white solid (127 mg, 65% yield) (decomposes at T> 170 °C). R_f 0.54 (cyclohexane/EtOAc, 6:4 v/v). ^{1}H NMR (300 MHz, DMSO-d_6): δ 7.45-7.33 (m, 5H), 7.20 (d, *J* = 9.0 Hz, 1H), 4.59 (m, 1H), 4.46 (s, 2H), 4.14 (m, 1H), 3.41 (dd, *J* = 10.5, 17.4 Hz, 1H), 3.27-3.16 (m, 2H), 3.10 (dd, *J* = 6.4, 17.4 Hz, 1H), 1.36 (s, 9H). ^{13}C NMR (75 MHz, DMSO-d_6): δ 155.6, 138.8, 131.5, 129.0, 128.9, 128.6, 82.4, 79.1, 59.2, 52.1, 47.6, 43.1, 28.6. $[\alpha]_D^{20}$ + 101.5 (*c* 0.55, DMSO).

tert-Butyl (*S*)-2-(benzylsulfonyl)-1-((*S*)-3-bromo-4,5-dihydroisoxazol-5-yl)ethylcarbamate (100 mg, 0.223 mmol) was treated with 15% TFA/DCM (2.2 mL, 10 eq) at room temperature for 1 h, then it was diluted with DCM and sat. aq. $NaHCO_3$ was added. Phases were separated and the

organic phase was dried over anhydrous Na_2SO_4, filtered and the solvent was removed under reduced pressure. The crude product was purified by flash chromatography on silica gel (cyclohexane/EtOAc, 4:6 v/v) obtaining (*S*)-2-(benzylsulfonyl)-1-((*S*)-3-bromo-4,5-dihydroisoxazol-5-yl)ethanamine [(α*S*,5*S*)-**3c**] as pale orange solid (54 mg, 70% yield) (m.p. 132.8-134.0°C). R_f 0.38 (cyclohexane/EtOAc, 4:6 v/v). ^{1}H NMR (300 MHz, $CDCl_3$): δ 7.42-7.38 (m, 5H), 4.55 (m, 1H), 4.33 (s, 2H), 3.55 (m, 1H), 3.25 (dd, *J* = 9.9, 17.4 Hz, 1H), 3.20 (dd, *J* = 8.1, 17.4 Hz, 1H), 3.13 (dd, *J* = 1.8, 14.1 Hz, 1H), 2.86 (dd, *J* = 9.3, 14.1 Hz, 1H), 2.18 (bs, 2H). ^{13}C NMR (75 MHz, $CDCl_3$): δ 137.9, 130.8, 129.2, 129.2, 127.5, 83.7, 60.9, 53.7, 49.0, 43.3. $[\alpha]_D^{20}$ + 116.3 (*c* 0.50, $CHCl_3$). MS(ESI): *m/z* calcd for $C_{12}H_{15}BrN_2O_3S$: 346.0; found: 347.1 $[M+H]^+$. Anal. calcd for $C_{12}H_{15}BrN_2O_3S$: C 41.51, H 4.35, N 8.07, found: C 41.43, H 4.51, N 7.95.

Synthesis of (*S*)-2-(benzylthio)-1-((*R*)-3-bromo-4,5-dihydroisoxazol-5-yl)ethanamine [(α*S*,5*R*)-4b]

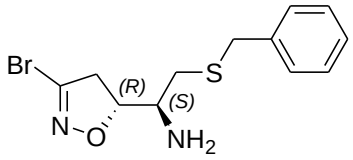

(α*S*,5*S*)-**4b**

(α*S*,5*R*)-**12** (390 mg, 0.939 mmol) was treated with 15% TFA/DCM (5.2 mL, 10 eq) at room temperature for 4 h, then it was diluted with DCM and the acid was quenched with 5% aq. $NaHCO_3$. Phases were separated and the aqueous phase was extracted with DCM. The pooled organic layers were dried over anhydrous Na_2SO_4, filtered and the solvent was removed under reduced pressure. The crude product was purified by flash chromatography on silica gel (cyclohexane/EtOAc, 2:8 v/v) obtained (*S*)-2-(benzylthio)-1-((*S*)-3-bromo-4,5-dihydroisoxazol-5-yl)ethan-1-amine [(α*S*,5*R*)-**4b**] as colourless oil, which solidifies upon cooling at − 20 °C (250 mg, 85% yield). R_f 0.44 (cyclohexane/EtOAc, 3:7 v/v). ^{1}H NMR (300 MHz, $CDCl_3$): δ 7.40-7.22 (m, 5H), 4.69 (ddd, *J* = 4.1, 8.8, 10.3 Hz, 1H), 3.73 (s, 2H), 3.18 (dd, *J* = 10.3, 17.1 Hz, 1H), 3.10 (dd, *J* = 8.8, 17.1 Hz, 1H), 2.75 (ddd, *J* = 4.1, 5.3, 8.4 Hz, 1H), 2.60 (dd, *J* = 5.3, 13.4 Hz, 1H), 2.43 (dd, *J* = 8.4, 13.4 Hz, 1H), 1.62 (bs, 2H). ^{13}C NMR (75 MHz, $CDCl_3$): δ 138.0, 137.7, 128.8, 128.6, 127.2, 83.6, 53.3, 43.9, 36.5, 36.4. $[\alpha]_D^{20}$ - 62.1 (*c* 0.43, $CHCl_3$). MS(ESI): *m/z* calcd for $C_{12}H_{15}BrN_2OS$: 314.0; found: 315.0 $[M+H]^+$. Anal. calcd for $C_{12}H_{15}BrN_2OS$: C 45.72, H 4.80, N 8.89, found: C 45.85, H 4.82, N 8.60.

Synthesis of (*S*)-2-(benzylsulfonyl)-1-((*R*)-3-bromo-4,5-dihydroisoxazol-5-yl)ethanamine [(α*S*,5*R*)-4c]

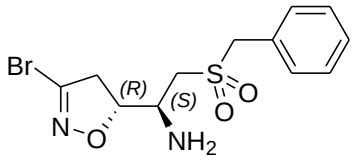

(α*S*,5*R*)-**4c**

*m*CPBA (131 mg, ≥77% purity, 0.583 mmol) was added at 0°C to a solution of (α*S*,5*R*)-**12** (110 mg, 0.265 mmol) in $CHCl_3$ (3.3 mL). Reaction mixture was stirred at room temperature for 10 min then DCM was added and washed with sat. aq. $NaHCO_3$. The organic phase was dried over anhydrous Na_2SO_4, filtered and the solvent was removed under reduced pressure, obtaining *tert*-butyl (*S*)-2-(benzylsulfonyl)-1-((*R*)-3-bromo-4,5-dihydroisoxazol-5-yl)ethylcarbamate as white solid (118 mg, quantitative yield) which recrystallizes from 1:3 v/v $CHCl_3$/EtOH as white needles (decomposes at T > 180°C). R_f 0.39 (cyclohexane/EtOAc, 7:3 v/v). ^{1}H NMR (300 MHz, $CDCl_3$): δ 7.46-7.37 (m, 5H), 5.00 (t, *J* = 9.4 Hz, 1H), 4.80 (d, *J* = 10.2 Hz, 1H), 4.42 (m, 1H), 4.34 (d, *J* = 14.2 Hz, 1H), 4.27 (d, *J* = 14.2 Hz, 1H), 3.33 (dd, *J* = 10.8, 17.7 Hz, 1H), 3.19-3.02 (m, 3H), 1.46 (s, 9H). ^{13}C NMR (75 MHz, $CDCl_3$): δ 155.5, 138.3, 130.7, 129.2, 129.1, 127.5, 81.9, 81.0, 60.1, 52.4, 48.4, 43.8, 28.2. $[\alpha]_D^{20}$ − 108.5 (*c* 0.55, $CHCl_3$).

tert-Butyl (*S*)-2-(benzylsulfonyl)-1-((*R*)-3-bromo-4,5-dihydroisoxazol-5-yl)ethylcarbamate (126 mg, 0.282 mmol) was treated with 15% TFA/DCM (2.8 mL, 10 eq) at room temperature for 1 h, then it was diluted with DCM and sat. aq. $NaHCO_3$ was added. The organic phase was separated and dried over anhydrous Na_2SO_4, filtered and the solvent was removed under reduced pressure. The crude product was purified by flash chromatography on silica gel (cyclohexane/EtOAc, 3:7 v/v) obtaining (*S*)-2-(benzylsulfonyl)-1-((*R*)-3-bromo-4,5-dihydroisoxazol-5-yl)ethanamine [(α*S*,5*R*)-**4c**] as white solid (67 mg, 68% yield) which recrystallizes from *i*PrOH as colorless needles (m.p. 144.6-145.5 °C). R_f 0.46 (cyclohexane/EtOAc, 3:7 v/v). ^{1}H NMR (300 MHz, CD_3OD): δ 7.49-7.38 (m, 5H), 4.73 (ddd, *J* = 4.0, 8.2, 10.5 Hz, 1H), 4.51 (s, 2H), 3.42 (ddd, *J* = 3.9, 4.0, 8.7 Hz, 1H), 3.34 (dd, *J* = 10.5, 17.4 Hz, 1H), 3.21 (dd, *J* = 8.6, 17.4 Hz, 1H), 3.21 (dd, *J* = 3.9, 14.7 Hz, 1H), 3.12 (dd, *J* = 8.7, 14.7 Hz, 1H). ^{13}C NMR (75 MHz, CD_3OD): δ 138.0, 130.9, 128.5, 128.4, 128.0, 83.8, 59.7, 54.4, 48.8, 42.8. $[\alpha]_D^{20}$ − 111.9 (*c* 0.50, MeOH). MS(ESI): *m/z* calcd for $C_{12}H_{15}BrN_2O_3S$: 346.0; found: 347.0 $[M+H]^+$. Anal. calcd for $C_{12}H_{15}BrN_2O_3S$: C 41.51, H 4.35, N 8.07, found: C 41.67, H 4.55, N 7.90.

1.3 Biological assays

Expression and purification of *Pf*GAPDH

Recombinant His-tagged *Pf*GAPDH was produced in *Escherichia coli*, as already described.[2]

Enzyme assays

GAPDH activity was evaluated using a modified version of the Ferdinand assay[5] in a buffered solution containing 10 mM TEA, 10 mM sodium arsenate, 5 mM EDTA, 1.5 mM NAD^+ and 2.2 mM DL-glyceraldehyde 3-phosphate, as already described.[2] GAPDH was added at a final concentration of 33 nM and NADH formation was monitored at 340 nm using a Cary4000 spectrophotometer (Agilent Technologies) with the cell holder maintained at 25 °C. The initial velocity was assessed by linear fitting of the initial phase of the kinetics.

Inhibition assays

A solution containing 2 μM *Pf*GAPDH, 10 mM TEA, 5 mM EDTA, 10 mM sodium arseniate, pH 7.6, was incubated at 25 °C in the presence of the inhibitors at various concentrations. Aliquots of the mixtures were periodically assayed for residual enzyme activity. The activity of aliquots of GAPDH maintained under the same conditions but in the absence of inhibitors was assayed as controls. The inhibition time courses were analyzed as biexponential decays[2] and the resulting inactivation rates (k_{obs}) at different inhibitor concentrations were analyzed with a Kitz-Wilson double reciprocal plot, performing a linear fitting with the equation:

$1/k_{obs}=Ki/k_{inact}[I]+1/k_{inact}$

The rate constant k_{inact} is associated to the covalent binding of the compound to the enzyme, K_i is the dissociation constant of the initial non-covalent enzyme-inhibitor complex and [I] is the concentration of the inhibitor. The k_{inact}/K_i ratio is the apparent second-order rate constant for inactivation and is indicative of the inhibitor reactivity.

Parasite Growth and Drug Susceptibility Assay

The CQ sensitive (D10) and CQ resistant (W2) strains of *P. falciparum* were sustained in vitro as described by Trager and Jensen.[6] All strains were cultured at 5% hematocrit (human type A-positive red blood cells) in RPMI 1640 (EuroClone, Celbio) medium with the addition of 1% AlbuMax (Invitrogen, Milan, Italy), 0.01% hypoxanthine, 20 mM Hepes Buffer, and 2 mM glutamine. Parasites were maintained at 37 °C in a standard gas mixture consisting of 1% O_2, 5% CO_2, and 94% N_2. For the drug sensitivity assay, compounds were dissolved in DMSO and then diluted with medium to achieve the required concentrations (final DMSO concentration <1%, which is nontoxic to the parasite). Drugs were placed in 96 well flat-bottom microplates (COSTAR) and serial dilutions made. Asynchronous cultures with parasitemia of 1–1.5% and 1% final hematocrit were

added into the plates and incubated for 72 h at 37 °C. Parasite growth was determined spectrophotometrically (OD_{650}) by measuring the activity of the parasite lactate dehydrogenase (pLDH), according to a modified version of Makler's method in control and drug-treated cultures.[7] Antiplasmodial activity is expressed as the 50% inhibitory concentrations (IC_{50}). Each IC_{50} value is the mean ± standard deviation of at least three separate experiments performed in duplicate.

Stability assay

The stability of one representative compound, chosen among those resulted inactive in the Drug Susceptibility Assay reported above, i.e. compound **4b**, was checked.

In detail 10 mg of compound **4b** were dissolved in 100 µL DMSO and added to 10 mL RPMI 1640 (EuroClone, Celbio) medium with the addition of 1% AlbuMax (Invitrogen, Milan, Italy), 0.01% hypoxanthine, 20 mM Hepes Buffer, and 2 mM glutamine. The solution was maintained at 37 °C in a standard gas mixture consisting of 1% O_2, 5% CO_2, and 94% N_2. After 72h, the solution was extracted with DCM (3 x 4 mL), the collected organic layers were washed with brine (1 x 4 mL), dried over anhydrous Na_2SO_4, filtered and the solvent was removed under reduced pressure. Compound **4b** was quantitatively recovered and its identity was confirmed by ^{1}H NMR analysis, by comparison with a pure sample.

Cytotoxicity Assay

The long-term human microvascular endothelial cell line (HMEC-1) immortalized by SV 40 large T antigen 38,[8] was maintained in MCDB 131 medium (GIBCO-BRL, Paisley, Scotland) supplemented with 10% fetal calf serum (HyClone, Logan, UT, USA), 10 ng/mL of epidermal growth factor (PreproTech, Rocky Hill, NY, USA), 1 µg/mL of hydrocortisone, 2 mM glutamine, 100 U/mL of penicillin, 100 µg/mL of streptomycin, and 20 mM Hepes buffer (EuroClone). For the cytotoxicity assays, HMEC-1 were treated with serial dilutions of test compounds for 72 h in a final volume of 200 µL/well and cell proliferation evaluated using the MTT assay. The results are expressed as IC_{50}, which is the dose of compound necessary to inhibit cell growth by 50%. Each IC_{50} value is the mean and standard deviation of at least three separate experiments performed in duplicate.

1.4 Molecular Modeling

Molecular modeling calculations were performed on E4 Server Twin 2 x Dual Xeon-5520, equipped with two nodes. Each node: 2 x Intel® Xeon® QuadCore E5520-2.26Ghz, 36 GB RAM. The molecular modeling graphics were carried out on a personal computer equipped with Intel(R) Core (TM) i7-4790 processor and SGI Octane 2 workstations.

Conformational analysis. The apparent pKa and logD values (pH 7.4 and 7.2) of the newly designed compounds were calculated by using the ACD/Percepta software (ACD/Percepta, Advanced Chemistry Development, Inc., Toronto, ON, Canada, 2017, http://www.acdlabs.com.) (Table 7SI). Accordingly, percentages of neutral/ionized forms were computed at pH 7.2 (cytoplasm) using the Henderson-Hasselbach equation. All the compounds were built taking into account the prevalent ionic forms at the considered pH value using the Small Molecule tool of Discovery Studio 2017 (Dassault Systèmes BIOVIA, San Diego, 2016). Then, the built compounds were subjected to molecular mechanic (MM) energy minimization (ε = 80*r) until the maximum RMS derivative was less than 0.001 kcal/Å, using Conjugate Gradient[9] as minimization algorithm (Discovery Studio 2017; Dassault Systèmes BIOVIA, San Diego, 2016). Atomic potentials and charges were assigned using the CFF forcefield.[10] The conformers obtained for each compound were used as starting structure for the subsequent systematic conformational analysis (Search Small Molecule Conformations; Discovery Studio 2017). The conformational space of the compounds was sampled by systematically varying the rotatable bonds sp3-sp3 and sp3-sp2 with an increment of 60°. The RMSD cutoff for structure selection was set to 0.01 (Å). Finally, to ensure a wide variance of the input structures to be successively fully minimized, an energy threshold value of 10^6 kcal/mol was used as selection criteria. The generated structures were then subjected to MM energy minimization (CFF forcefield; ε = 80*r) until the maximum RMS derivative was less than 0.001 kcal/Å, using Conjugate Gradient as minimization algorithm. Finally, the resulting conformers were ranked by their potential energy values (i.e., ΔE from the global energy minimum) and grouped into conformational families on the basis of dihedral angle values.

Bioinformatics Analysis. The experimentally determined structures of (i) human GAPDH (PDB IDs: 1U8F, 1ZNQ, 3GPD, 3H9E, 3PFW, 4WNC, 4WNI, 5C7L and 5C7O), (ii) *Plasmodium falciparum* GAPDH (PDB IDs: 1YWG, 2B4R and 2B4T), and (iii) *Trypanosoma Cruzi* GAPDH (PDB ID: 1ML3), were downloaded from the Protein Data Bank (PDB; http://www.rcsb.org/pdb/). Hydrogens were added to all the PDB structures assuming a pH of 7.2. These structures were analyzed using Macromolecules and Receptor-Ligand Interaction tools of Discovery Studio 2017.

Modeling of Pf GAPDH. Since all *Pf* GAPDH experimentally determined structures are incomplete, the molecular model of *Pf* GAPDH was built. All subsequent structural calculations were performed using the CVFF force field.[11]

The molecular model of *Pf* GAPDH was built starting from the experimentally determined structure of *Pf* GAPDH (PDB ID: 1YWG), which lacks the side chains of several residues (D39, N41, D64, E106, D127, K222, E226, N228, K254 and E259). The sequence of 1YWG was aligned with the sequences of *Pf* GAPDH downloaded from the UniProtKB/Swiss-Prot Data Bank (http://www.uniprot.org; entry Q8T6B1) by using the Multiple_Alignment algorithm (Homology module, Accelrys, San Diego). The coordinates were assigned by the Structurally Conserved Regions (SCRs)-AssignCoords procedure (Homology Module, Insight 2005) using 1YWG as template structure. The obtained homology model was completed inserting i) the missing residue side chains by using the Replace command (Biopolymer module, Accelrys, San Diego) and ii) the four molecules of NAD^+ present in the experimentally determined structure of *Pf* GAPDH (PDB ID: 1YWG) through the Modify/UnMerge and Modify/Merge commands (Biopolymer module, Accelrys, San Diego).

The obtained homology model was then subjected to a full energy minimization within Insight 2005 Discover_3 module (Steepest Descent algorithm, maximum RMS derivative = 0.5 kcal/Å; ε = 80*r). The partial charges to NAD^+ molecules were assigned by MNDO semiempirical 1SCF calculation.[12] During the minimization, only the SCRs side chains were left free to move, whereas the SCRs backbone were fixed to avoid unrealistic results. The quality of the resulting complexes was then checked using Molprobity structure evaluator software[13] and compared to that of the reference PDB structure. The obtained homology model was used for successive dynamic docking studies.

Docking studies. In order to find the bioactive conformation, docking studies were carried out on **1b**, **1c**, **2a**, **3c**, and **4** in complex with *Pf* GAPDH. Although in the subsequent dynamic docking protocol all the systems were perturbed by a Monte Carlo/minimization procedure, nevertheless the dynamic docking procedure formally requires a reasonable starting structure. In order to define the starting conformation of new compounds, all conformers of **1b**, **1c**, **2a**, **3c**, and **4** within 5 kcal/mol from the global minimum were placed in GAPDH catalytic site taking into account the two binding modes of the glyceraldehyde 3-phosphate analogue 2-(2-phosphono-ethyl)-acrylic acid 4-nitro-phenyl ester (PDB ID: 1ML3). In particular, the electrophilic carbon and the nitrogen atom of 3-Br-isoxazoline ring were superimposed on the carbonyl group of glyceraldehyde 3-phosphate analogue as well as the carbonyl group or the sulfur atom on the phosphate atoms. The conformations with

the lowest potential energy that did not show significant steric overlap with catalytic-site amino acids were selected as starting conformations for the docking calculations.

The putative starting complexes were subjected to dynamic docking studies (Affinity, SA_Docking; Insight2005, Accelrys, San Diego). In particular, a Monte Carlo/minimization approach, which considers all the systems flexible (i.e., ligand and protein), was used. Flexible docking was achieved using the Cell Multipole method for nonbond interactions.

The binding domain area was defined as a subset including all residues of *Pf*GAPDH. All atoms included in the binding domain area were left free to move during the entire course of docking calculations, whereas, in order to investigate the first approach of our newly designed compounds to the catalytic site before the nucleophilic attack, a tethering restraint was applied on: i) the hydrogen bond between the catalytic residues C153 and H180 (constrained within 2.5 Å using a force constant of 100 (kcal/mol)/Å) and ii) the distance between the electrophilic carbon of 3-Br-isoxazoline ring and the sulfur atom of C153. In particular, this distance was constrained in the range from 3.0 Å to 3.4 Å using a force constant of 100 (kcal/mol)/Å according to the data present in the literature.[14] Moreover, in order to avoid unrealistic results, a tethering restraint was applied on the Structurally Conserved Regions (SCRs) of protein. To identify SCRs, the *Pf*GAPDH sequence was analyzed using the Structure Prediction and Sequence Analysis server PredictProtein (http://www.predictprotein. org/). In *Pf*GAPDH, 8 α-helix and 17 β-sheet secondary structures were predicted to be highly conserved (α1, aa13−23; α2, aa40−48; α3, aa105−113; α4, aa155−167; α5, aa198−207; α6, aa214−227; α7, aa258-270; α8, aa323-335 β1, aa4-8; β2, aa29-34; β3, aa58−62; β4, aa66−70; β5, aa73−79; β6, aa93-98; β7, aa118-123; β8, aa131-136; β9, aa146-149; β10, aa171-182; β11, aa234-238; β12, aa244-252; β13, aa275-278; β14, aa284-288; β15, aa296-299; β16, aa303-306; β17, aa310-317). Accordingly, for the alpha-helices, the distance between backbone hydrogen bond donors and acceptors was restrained within 2.5 Å. On the other hand, for the beta-sheets, the φ and ψ torsional angles, according to the parallel or anti-parallel conformation, were restrained within -119° and +113°, or -139° and +135°, respectively (Restrain command; Discover_3 module, Accelrys, San Diego). According to the reliability index values obtained from the secondary structure prediction analysis, we applied restraints with a quadratic form and the following set of force constants: i) 1 kcal/mol/Å^2 (maximum force: 10 kcal/mol/Å^2) for reliability index values from 0 to 3, ii) 10 kcal/mol/Å^2 (maximum force: 100 kcal/mol/Å^2) for reliability index values from 4 to 6, and iii) 100 kcal/mol/Å^2 (maximum force: 1000 kcal/mol/Å^2) for reliability index values from 7 to 9.

The docking protocol included a Monte Carlo-Metropolis based conformational search of the ligand within the obtained homology model of *Pf*GAPDH for the random generation of a maximum of 20

acceptable complexes. During the first step, starting from the previously obtained roughly docked structures, the ligand was moved by a random combination of translation, rotation, and torsional changes to sample both the conformational space of the ligand and its orientation with respect to the protein (MxRChange = 3 Å; MxAngChange = 180°). During this step, van der Waals (vdW) and Coulombic terms were scaled to a factor of 0.1 to avoid very severe divergences in the vdW and Coulombic energies. If the energy of a complex structure resulting from random moves of the ligand was higher by the energy tolerance parameter than the energy of the last accepted structure, it was not accepted for minimization. To ensure a wide variance of the input structures to be successively minimized, an energy tolerance value of 10^6 kcal/mol from the previous structure was used. After the energy minimization step (conjugate gradient; 2500 iterations; $\varepsilon = 1$), the energy test, with an energy range of 50 kcal/mol, and a structure similarity check (rms tolerance = 0.3 kcal/Å) was applied to select the 20 acceptable structures. Each subsequent structure was generated from the last accepted structure. Following this procedure, the resulting docked structures were ranked by their conformational energy and were analyzed considering the non-bonded interaction energies between the ligand and the enzyme (vdW and electrostatic energy contribution; Group Based method; CUT_OFF = 100; $\varepsilon = 2*r$; Discover_3 Module of Insight2005). The complex with the best non-bond interaction energy was selected as the structure representing the most probable binding mode. In order to allow the whole relaxation of the protein and the ligand, the selected docked complexes were then subjected to MM energy minimization without restraints (Steepest Descent algorithm; $\varepsilon = 1$) until the maximum RMS derivative was less than 0.1 kcal/Å (Module Discover; Insight 2005). The resulting structures were analyzed considering the non-bonded interaction energies between the ligand and the enzyme (vdW and electrostatic energy contribution; Group Based method; CUT_OFF = 100; $\varepsilon = 2*r$; Discover_3 Module of Insight2005).

The putative bioactive conformers of **2a-d** have been subjected to a single point (SP) DFT calculation. The calculations were carried out using the Gaussian 09 package.[15] All structures were optimized at the B3LYP/6-31+G(d,p) level[16-17] using the conductor-like polarizable continuum model (C-PCM).[18] The C-PCM method allows the calculation of the energy in the presence of a solvent. In this case all structures were optimized as a solute in an aqueous solution. The atomic charges have been calculated using the natural bond orbital (NBO) method.[19] The atomic charges, derived from the NBO population analysis, were used to calculate the dipole moment of the (substituted)-phenyl ring (Module Decipher, Insight 2005).

2. References

1. Conti, P.; Pinto, A.; Wong, P. E.; Major, L. L.; Tamborini, L.; Iannuzzi, M. C.; De Micheli, C.; Barrett, M. P.; Smith, T. K. Synthesis and in vitro/in vivo evaluation of the antitrypanosomal activity of 3-bromoacivicin, a potent CTP synthetase inhibitor. *ChemMedChem* **2011**, *6*, 329-333.

2. Bruno, S.; Pinto, A.; Paredi, G.; Tamborini, L.; De Micheli, C.; La Pietra, V.; Marinelli, L.; Novellino, E.; Conti, P.; Mozzarelli, A. Discovery of covalent inhibitors of glyceraldehyde-3-phosphate dehydrogenase, a target for the treatment of malaria. *J. Med. Chem.* **2014**, *57*, 7465-7471;

3. Daniels, R. N.; Melancon, B. J.; Wang, E. A.; Crews, B. C.; Marnett, L. J.; Sulikowski, G. A.; Lindsley, C. W. Progress toward the total synthesis of lucentamycin A: total synthesis and biological evaluation of 8-*epi*-lucentamycin A. *J. Org. Chem.* **2009**, *74*, 8852-8855;

4. Trost, B. M.; O'Boyle; B. M.; Torres W.; Ameriks, M. K. Development of a flexible strategy towards FR900482 and the mitomycins. *Chem. Eur. J.* **2011**, *17*, 7890-7903.

5. Ferdinand, W. The isolation and specific activity of rabbit-muscle glyceraldehyde phosphate dehydrogenase. *Biochem J.* **1964**, *92*, 578-585.

6. Imperatore, C.; Persico, M.; Aiello, A.; Luciano, P,; Guiso, M.; Sanasi, M. F.; Taramelli, D.; Parapini, S.; Cebrian-Torrejon, G.; Domenech-Carbo, A.; Fattorusso, C.; Menna, M. Marine inspired antiplasmodial thiazoquinones: synthesis, computational studies and electrochemical assays**.** *RSC Adv.*, **2015**, *5*, 70689-70702.

7. Makler, M. T.; Ries, J. M.; Williams, J. A.; Bancroft, J. E.; Piper, R. C.; Gibbins, B. L.; Hinrichs, D. Parasite lactate dehydrogenase as an assay for *Plasmodium falciparum* drug sensitivity. *Am. J. Trop. Med. Hyg.* **1993**, *48*, 739–741.

8. Basilico, N.; Corbett, Y.; D'Alessandro, S.; Parapini, S.; Prato, M.; Girelli, D.; Misiano, P.; Olliaro, P.; Taramelli, D. Malaria pigment stimulates chemokine production by human microvascular endothelium. *Acta Tropica* **2017**, *172*, 125-131.

9. Fletcher, R. Unconstrained optimization. In Practical Methods of Optimization, 1st ed.; John Wiley & Sons Ltd.: New York, NY, USA, 1980; Vol. 1, pp. 1–128, ISBN 978-0471277118.

10. Ewig, C. S.; Berry, R.; Dinur, U.; Hill, J. R.; Hwang, M. J.; Li, H.; Liang, C.; Maple, J.; Peng, Z.; Stockfisch, T. P.; Thacher, T. S.; Yan, L.; Ni, X.; Hagler, A.T. Derivation of class II force fields. VIII. Derivation of a general quantum mechanical force field for organic compounds. *J. Comput. Chem.* **2001**, *22*, 1782-1800.

11. Dauber-Osguthorpe, P.; Roberts, V.A.; Osguthorpe, D.J.; Wolff, J.; Genest, M.; Hagler, A.T. Structure and energetics of ligand binding to proteins: *Escherichia coli* dihydrofolate reductase-trimethoprim, a drug-receptor system. *Proteins* **1988**, *4*, 31-47.

12. Dewar, M. J. S.; Thiel, W. Ground states of molecules. 38. The MNDO method. Approximations and parameters, *J. Am. Chem. Soc*. **1977**, *99*, 4899-4907.

13. Davis, I.W.; Leaver-Fay, A.; Chen, V. B.; Block, J. N.; Kapral, G. J.; Wang, X.; Murray, L. W.; Arendall, W.B.; Snoeyink, J.; Richardson, J.S.; Richardson, D.C. MolProbity: all-atom contacts and structure validation for proteins and nucleic acids. *Nucleic Acids Res.* **2007**, *35*, W375-W383.

14. a. Lodola, A.; Branduardi, D.; De Vivo, M.; Capoferri, L.; Mor, M.; Piomelli, D.; Cavalli, A. A catalytic mechanism for cysteine *N*-terminal nucleophile hydrolases, as revealed by free energy simulations. *PLoS One* **2012**, 7(2):e32397. B. Arafet, K.; Ferrer, S.; González, F. V.; Moliner, V. Quantum mechanics/molecular mechanics studies of the mechanism of cysteine protease inhibition by peptidyl-2,3-epoxyketones. *Phys Chem Chem Phys*. **2017**, *19*, 12740-12748.

15. Gaussian 09, Revision D.01, Frisch, M. J.; Trucks, G. W.; Schlegel, H. B.; Scuseria, G. E.; Robb, M. A.; Cheeseman, J. R.; Scalmani, G.; Barone, V.; Mennucci, B.; Petersson, G. A.; Nakatsuji, H.; Caricato, M.; Li, X.; Hratchian, H. P.; Izmaylov, A. F.; Bloino, J.; Zheng, G.; Sonnenberg, J. L.; Hada, M.; Ehara, M.; Toyota, K.; Fukuda, R.; Hasegawa, J.; Ishida, M.; Nakajima, T.; Honda, Y.; Kitao, O.; Nakai, H.; Vreven, T.; Montgomery, J. A., Jr.; Peralta, J. E.; Ogliaro, F.; Bearpark, M.; Heyd, J. J.; Brothers, E.; Kudin, K. N.; Staroverov, V. N.; Kobayashi, R.; Normand, J.; Raghavachari, K.; Rendell, A.; Burant, J. C.; Iyengar, S. S.; Tomasi, J.; Cossi, M.; Rega, N.; Millam, N. J.; Klene, M.; Knox, J. E.; Cross, J. B.; Bakken, V.; Adamo, C.; Jaramillo, J.; Gomperts, R.; Stratmann, R. E.; Yazyev, O.; Austin, A. J.; Cammi, R.; Pomelli, C.; Ochterski, J. W.; Martin, R. L.; Morokuma, K.; Zakrzewski,V. G.; Voth, G. A.; Salvador, P.; Dannenberg, J. J.; Dapprich, S.; Daniels, A. D.; Farkas, Ö.; Foresman, J. B.; Ortiz, J. V.; Cioslowski, J.; Fox, D. J. Gaussian, Inc., Wallingford CT, **2009**.

16. Becke, A. D. Density-functional thermochemistry. III. The role of exact exchange. *J. Chem. Phys.* **1993**, *98*, 5648−5652.

17. Lee, C.; Yang, W.; Parr, R. G. Development of the Colle-Salvetti correlation-energy formula into a functional of the electron density. *Phys. Rev. B: Condens. Matter Mater. Phys.* **1988**, *37*, 785-789.

18. Cossi, M.; Rega, N.; Scalmani, G.; Barone, V. Energies, structures, and electronic properties of molecules in solution with the C-PCM solvation model. *J. Comp. Chem.* **2003**, *24*, 669-681.

19. Reed, A. E.; Weinstock, R. B.; Weinhold, F. Natural Population Analysis. *J. Chem. Phys.* **1985**, *83*, 735-746.

3. Figures

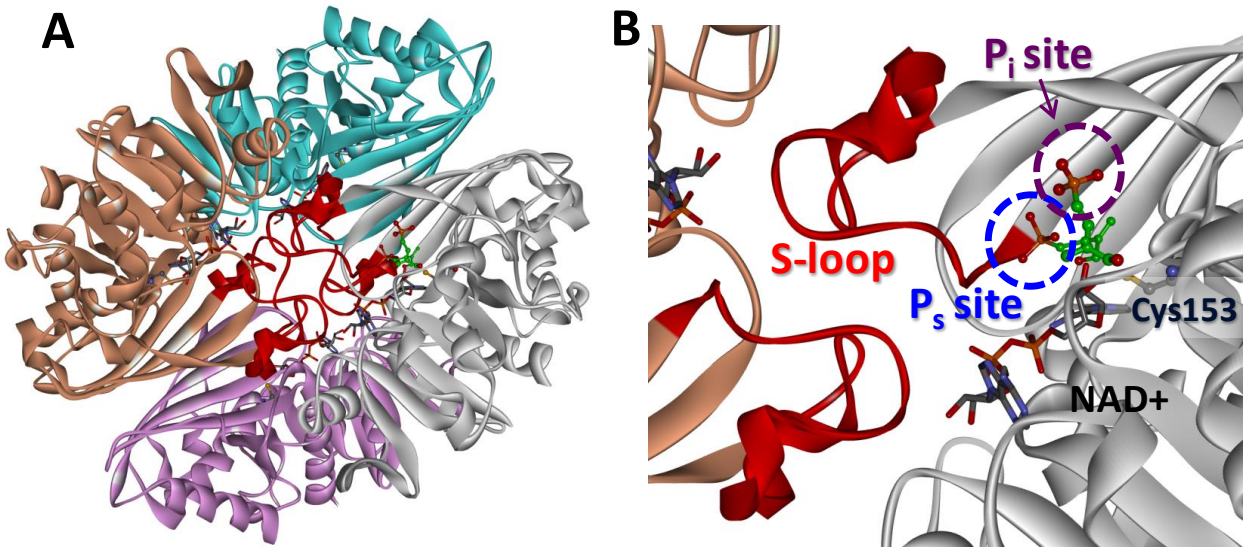

Figure 1SI. A) X-ray structure of tetrameric form of *Pf*GAPDH (PDB ID: 1YWG). B) Zoom of the catalytic site *Pf*GAPDH. The four monomers of *Pf*GAPDH are displayed as solid ribbons and colored in pink, white, light brown and cyan. The S-loop (181-209) of each monomer is colored in red. The reacted irreversible inhibitor 2-(2-phosphono-ethyl)-acrylic acid 4-nitro-phenyl ester (green and ball&stick; PDB ID: 1LM3), the catalytic cysteine (gray and ball&stick) and NAD^+ (gray and stick) are colored by atom type: (N: blue; O: red; P: orange; S:yellow).

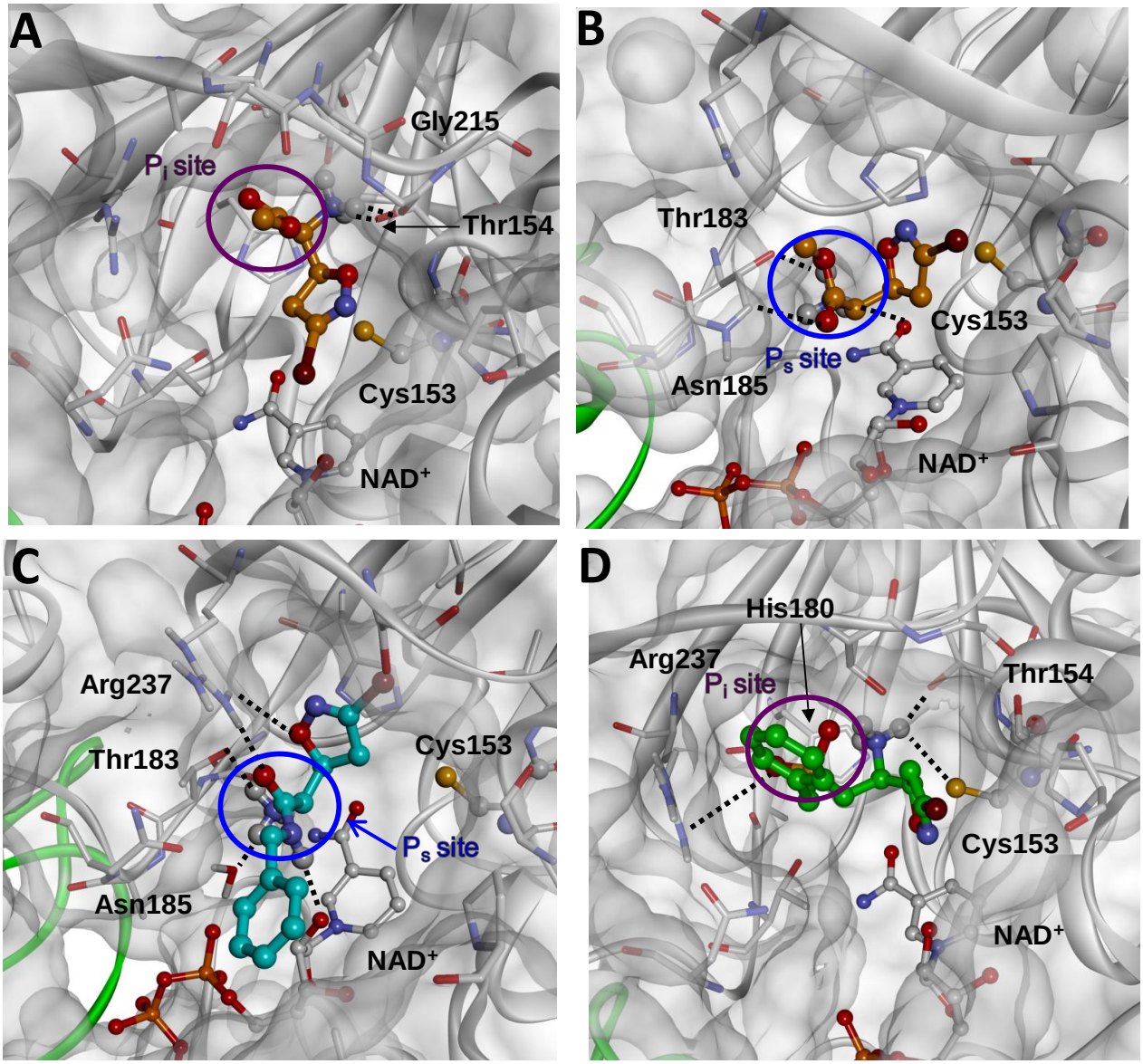

Figure 2SI. Overview of **1b** (orange) bound to P_i site (A) and P_s site (B) of *Pf*GAPDH. C) Overview of **2a** (cyan) bound to P_s site of *Pf*GAPDH. D) Overview of **4c** (green) bound to P_i site of *Pf*GAPDH. The protein (gray) is displayed as Connolly surface and solid ribbons; the second monomer is colored in green. The ligands, NAD^+ and Cys153 (ball&stick) as well as the residues involved in the interactions with ligands (stick) are colored by atom type (N: blue; O: red; P: orange; S:yellow; Br: brown).

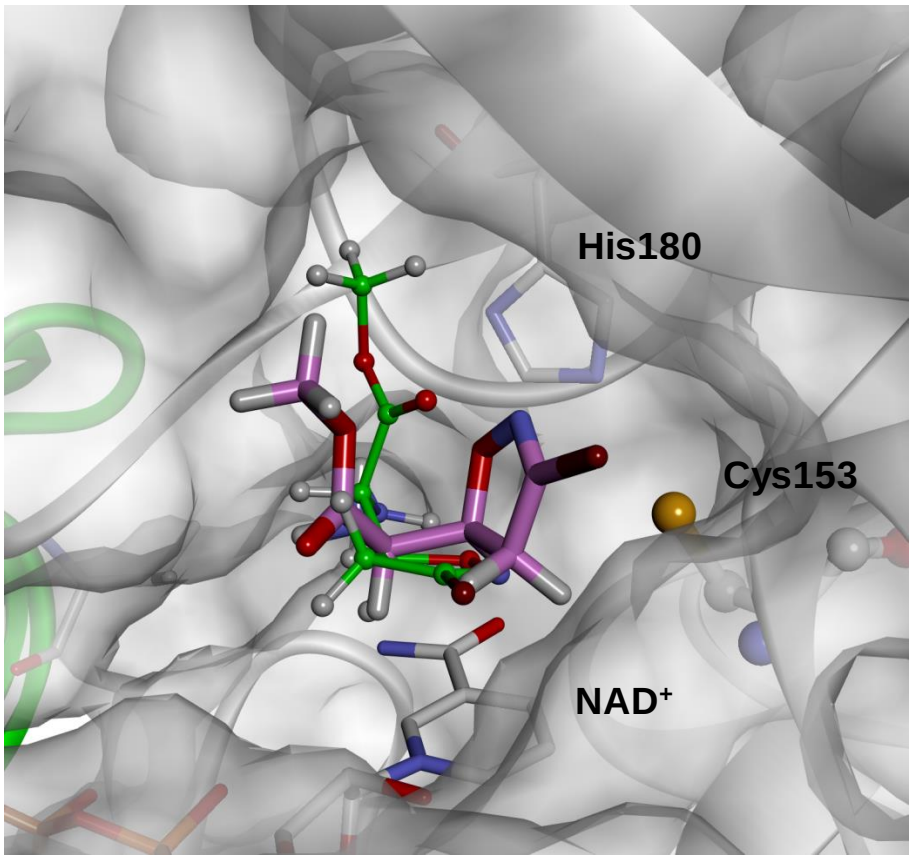

Figure 3SI. Superimposition of the binding modes of **1b** in the catalytic site of *Pf*GAPDH obtained after the docking studies (pink and stick) and after Molecular Mechanics energy minimization without any restraint (green and ball&stick). *Pf*GAPDH is displayed as Connolly surface and colored in gray. The ligands, NAD^+, Cys153 and His180 are colored by atom type (N: blue; O: red; P: orange; S:yellow).

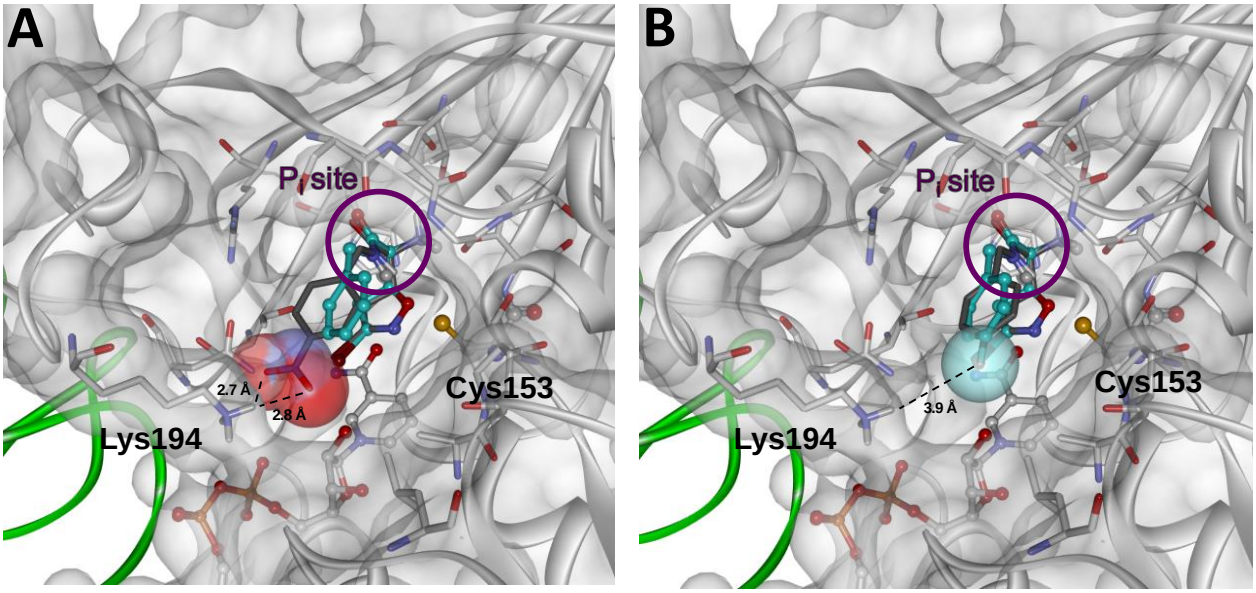

Figure 4SI. Superimposition of **2d** (gray; A) and **2c** (gray; B) on **2a** (cyan) bound to P_i site of *Pf*GAPDH (bioactive approach; Complex 1 in Table 3SI; Figure 1C) . The protein (gray) is displayed as Connolly surface and solid ribbons; the second monomer is colored in green. The ligand **2a**, NAD^+ and Cys153 (ball&stick) as well as the residues involved in the interactions with ligands (stick) are colored by atom type (N: blue; O: red; P: orange; S:yellow; Br: brown). The van der Waals volumes of the nitro group and the fluorine atom are displayed as transparent surface and colored by atom type; the interatomic distances for the putative hydrogen bonds of **2d** and **2c** with Lys194 are reported and evidenced by black dashed lines.

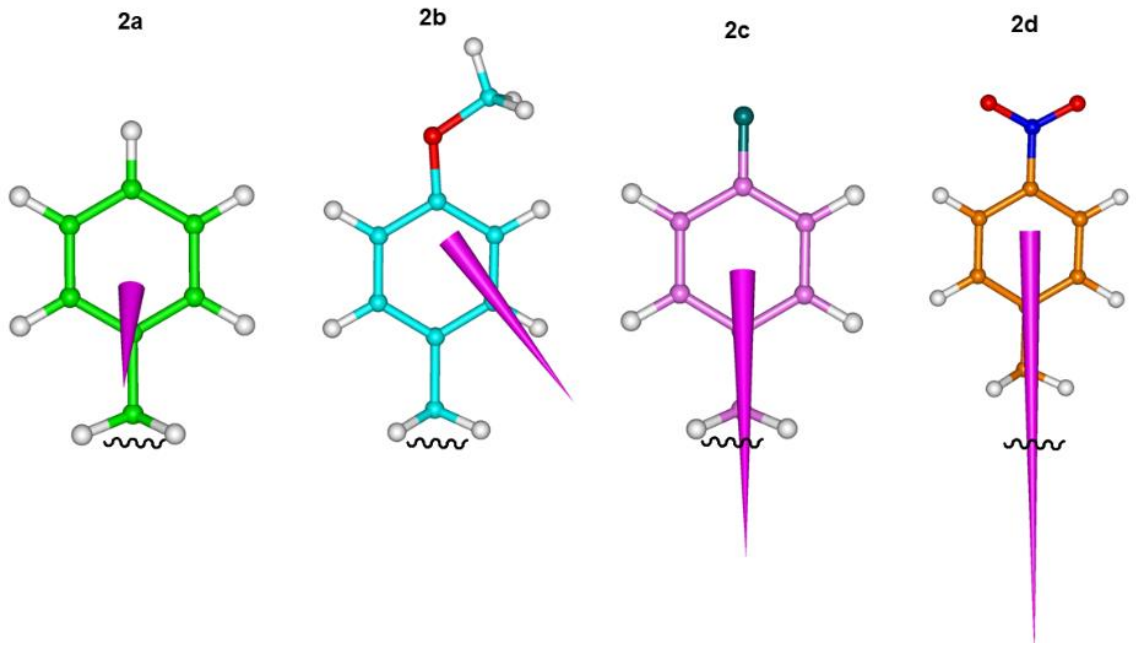

Figure 5SI. Calculated dipole moments of the (substituted)-phenyl ring of **2a-d**. Charges were calculated using the natural bond orbital (NBO) method, after DFT minimization at the B3LYP/6-31+G(d,p) level using the conductor-like polarizable continuum model (C-PCM) (see the Experimental Section for details). Heteroatoms are colored by atom type (N: blue; O: red; P: orange; S:yellow); the dipole vector is displayed as a solid cone and colored in magenta.

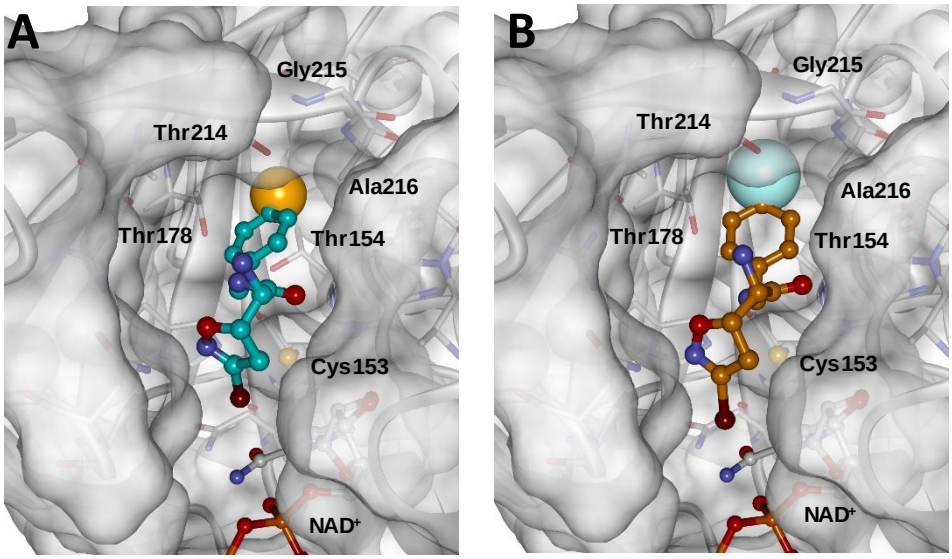

Figure 6SI. A: Complex 3 of GAPDH-**2a** generated by the Monte Carlo/Minimization docking procedure (see Table 3SI). In this binding mode the phenyl ring occupies the same binding cleft occupied by the NH_2 group in the bioactive binding mode (Complex 1 in Table 3SI; Figure 1C). B: low energy conformer of **2c** (orange; ΔE_{GM}: 0.9 kcal/mol) superimposed on the docked conformation of **2a** reported in A. The fluorine atom could establish additional H-bond interactions with the surrounding threonine residues thus reproducing the interactions of the NH_2 function of **2a** in Complex 1 (reported in Figure 1 C). The protein (gray) is displayed as Connolly surface and solid ribbons. The ligands, NAD^+ and Cys153 as well as the residues lining the pocket interacting with phenyl ring are labelled and colored by atom type (N: blue; O: red; P: orange; S: yellow; Br: brown). The van der Waals volumes of the para-hydrogen of **2a** (orange) and the fluorine atom of **2c** (cyan) are displayed.

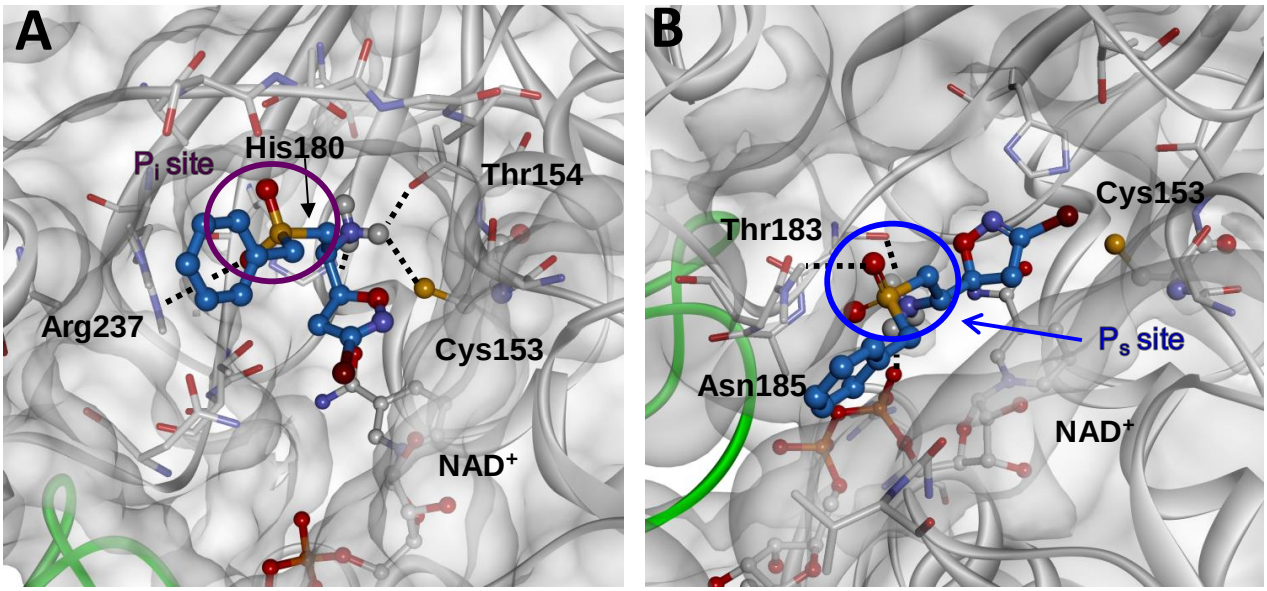

Figure 7SI. Overview of **3c** (orange) bound to P_i site (A) and P_s site (B) of *Pf*GAPDH. The protein (gray) is displayed as Connolly surface and solid ribbons; the second monomer is colored in green. The ligands, NAD^+ and Cys153 (ball&stick) as well as the residues involved in the interactions with ligands (stick) are colored by atom type (N: blue; O: red; P: orange; S: yellow; Br: brown).

D10

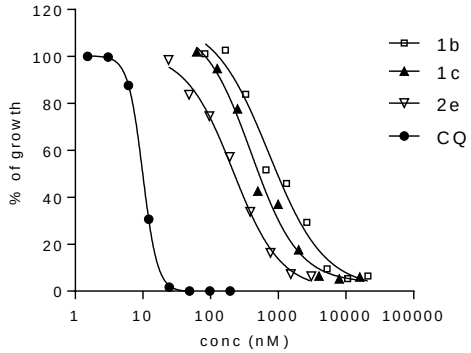

W2

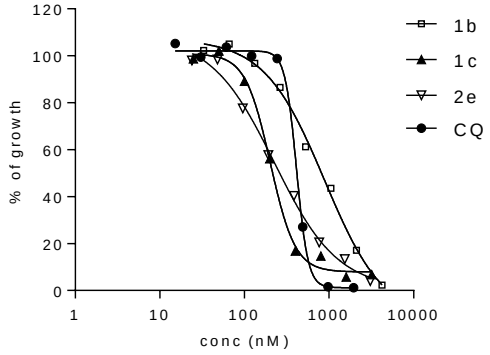

Figure 8SI. Dose-response curves of compounds **1b**, **1c**, **2e** and **CQ** against *P. falciparum* strain D10 or W2. The data are the results of a representative experiment in duplicate conducted using the pLDH assay. See above for details of the chemosensitivity assay.

4. Tables

Table 1SI. Non-bonded interaction energies (kcal/mol) of the GAPDH-**1b** complexes obtained by Monte Carlo/Minimization procedure.

Cplx	**Non-bonded interaction energies (kcal/mol)**					
	Starting from P_i site			Starting from P_s site		
	Total	VdW	Coulomb	Total	VdW	Coulomb
1	-6,456	-9,087	2,631	-4,059	-6,360	2,301
2	5,676	-1,911	7,588	7,461	5,161	2,300
3	6,487	2,960	3,527	-0,304	-5,350	5,045
4	13,313	8,226	5,087	-3,161	-6,457	3,296
5	-3,426	-7,066	3,640	4,445	-1,494	5,938
6	79,200	79,373	-0,173	25,054	23,336	1,718
7	28,746	33,563	-4,816	12,736	13,509	-0773
8	37,448	39,402	-1,954	17,483	17,138	0,345

Table 2SI. Non-bonded interaction energies (kcal/mol) of the GAPDH-**1c** complexes obtained by Monte Carlo/Minimization procedure.

Cplx	**Non-bonded interaction energies (kcal/mol)**					
	Starting from P_i site			Starting from P_s site		
	Total	VdW	Coulomb	Total	VdW	Coulomb
1	-7,548	-10,132	2,585	-8,943	-10,405	1,462
2	-1,630	-6,244	4,614	-3,476	-7,707	4,231
3	8,123	0,489	7,634	-2,418	-8,343	5,925
4	-0,0,96	-3,742	3,646	21,830	18,514	3,316
5	3,763	-0,367	4,130	20,578	17,634	2,945
6	43,707	46,405	-2,698	65,453	63,603	1,849
7	-	-	-	57,282	58,940	-1,658
8	-	-	-	-4,548	-1,296	-3,253

Table 3SI. Non-bonded interaction energies (kcal/mol) of the GAPDH-**2a** complexes obtained by Monte Carlo/Minimization procedure.

Cplx	Non-bonded interaction energies (kcal/mol)					
	Starting from P_i site			Starting from P_s site		
	Total	VdW	Coulomb	Total	VdW	Coulomb
1	-7,193	-9,795	2,601	-8,592	-10,069	1,478
2	-1,133	-4,479	3,346	-1,674	-5,233	3,560
3	7,825	3,753	4,072	-2,000	-4,968	2,968
4	11,784	9,392	2,392	8,792	2,472	6,320
5	0,382	-2,733	3,115	0,468	-3,876	4,344
6	31,489	32,811	-1,322	33,031	36,680	-3,649
7	27,649	29,313	-1,664	12,445	14,615	-2,170
8	-	-	-	8,165	10,312	-2,147

Table 4SI. Non-bonded interaction energies (kcal/mol) of the GAPDH-**3c** complexes obtained by Monte Carlo/Minimization procedure.

Cplx	Non-bonded interaction energies (kcal/mol)					
	Starting from P_i site			Starting from P_s site		
	Total	VdW	Coulomb	Total	VdW	Coulomb
1	-8,994	-11,437	2,444	-5,858	-6,989	1,131
2	11,138	7,201	3,937	9,452	7,992	1,460
3	33,278	27,763	5,514	18,309	13,801	4,508
4	4,579	2,391	2,188	-0,317	-2,117	1,800
5	-2,823	-7,246	4,422	-2,338	-4,855	2,517
6	20,027	22,850	-2,823	74,180	79,391	-5,210
7	0,218	2,626	-2,408	31,303	34,441	-3,138
8	-	-	-	41,606	43,706	-2,099

Table 5SI. Non-bonded interaction energies (kcal/mol) of the GAPDH-**4** complexes obtained by Monte Carlo/Minimization procedure.

Cplx	Non-bonded interaction energies (kcal/mol)					
	Starting from P_i site			Starting from P_s site		
	Total	VdW	Coulomb	Total	VdW	Coulomb
1	-8,120	-11,538	3,418	-6,195	-8,305	2,110
2	-0,549	-3,231	2,683	-1,123	-5,270	4,146
3	-5,304	-8,849	3,545	15,845	12,332	3,514
4	-3,598	-3,567	-0,031	32,836	28,724	4,112
5	-2,717	0,553	-3,269	-1,544	-5,259	3,715
6	47,922	50,587	-2,665	-	-	-
7	20,329	20,329	0,001	-	-	-
8	10,152	9,930	0,222	-	-	-

Table 6SI. Non-bonded interaction energies (kcal/mol) of the selected docked complexes

Cplx	Non-bonded interaction energies (kcal/mol)					
	Starting from P_i site			Starting from P_s site		
	Total	vdW	Coulomb	Total	vdW	Coulomb
GAPDH-1b	-17,168	-12,526	-4,643	-4,059	-6,360	2,301
GAPDH-1c	-21,009	-19,280	-1,729	-16,176	-13,175	-3,002
GAPDH-2a	-20,792	-16,564	-4,228	-17,390	-13,998	-3,393
GAPDH-3c	-19,892	-17,086	-2,805	-13,467	-12,552	-0,916
GAPDH-4	-19,822	-17,822	-2,000	-16,584	-12,677	-3,907

Table 7SI. cLogD and percentage of Ionic Forms.

Compd	$cLogD_{7.4}$	Prevalent Ionic Form (%)	
		pH 7.4	pH 7.2
1a	0.02	ZW (100)	ZW(100)
1b	0.04	N (61) P(39)	N(49) P(51)
1c	1.41	N(64) P(36)	N(53) P(47)
2a	0.76	N(50) P(50)	N (39) P(61)
2b	0.65	N(48) P(52)	N (37) P(63)
2c	0.92	N(50) P(50)	N (39) P(61)
2d	0.80	N(54) P(46)	N (43) P(57)
2e	0.97	N(46) P(54)	N (35) P(65)
3a	0.65	N(3) P(97)	N(2) P(98)
3b	1.00	N(3) P(97)	N(2) P(98)
3c	0.62	N(48) P(52)	N (36) P(64)
4	0.62	N(48) P(52)	N (36) P(64)